# 2′-Deoxy-3′-*O*-(4-benzoylbenzoyl)- and 3′(2′)-*O*-(4-Benzoylbenzoyl)-1,$N^6$-ethenoadenosine 5′-Diphosphate, Fluorescent Photoaffinity Analogues of Adenosine 5′-Diphosphate. Synthesis, Characterization, and Interaction with Myosin Subfragment 1†

Christine R. Cremo*,‡ and Ralph G. Yount

*Biochemistry/Biophysics Program, Institute of Biological Chemistry, and Department of Chemistry, Washington State University, Pullman, Washington 99164-4660*

*Received February 13, 1987; Revised Manuscript Received May 14, 1987*

ABSTRACT: Two new fluorescent nucleotide photoaffinity labels, 3′(2′)-*O*-(4-benzoylbenzoyl)-1,$N^6$-ethenoadenosine 5′-diphosphate ($Bz_2\epsilon$ADP) and 2′-deoxy-3′-*O*-(4-benzoylbenzoyl)-1,$N^6$-ethenoadenosine 5′-diphosphate [3′($Bz_2$)2′dεADP], have been synthesized and used as probes of the ATP binding site of myosin subfragment 1 ($SF_1$). These analogues are stably trapped by the bifunctional thiol cross-linker *N*,*N*′-*p*-phenylenedimaleimide (pPDM) at the active site in a manner similar to that of ATP [Wells, J. A., & Yount, R. G. (1979) *Proc. Natl. Acad. Sci. U.S.A. 76*, 4966–4970], and nonspecific photolabeling can be minimized by removing free probe by gel filtration prior to irradiation. Both probes covalently photoincorporate with high efficiency (40–50%) into the central 50-kDa heavy chain tryptic peptide, as found previously for the nonfluorescent parent compound 3′(2′)-*O*-(4-benzoylbenzoyl)adenosine diphosphate [Mahmood, R., & Yount, R. G. (1984) *J. Biol. Chem. 259*, 12956–12959]. The solution conformations of $Bz_2\epsilon$ADP and 3′($Bz_2$)-2′dεADP were analyzed by steady-state and time-resolved fluorescence spectroscopy. These data indicated that the benzoylbenzoyl rings in both analogues were stacked over the ε-adenine ring. The degree of stacking was greater with the 2′ isomer than with the 3′ isomer. Fluorescence quantum yields and lifetimes were measured for $Bz_2\epsilon$ADP and 3′($Bz_2$)2′dεADP reversibly bound, stably trapped, and covalently photoincorporated at the active site of $SF_1$. These values were compared with those for 3′(2′)-*O*-[[(phenylhydroxymethyl)phenyl]carbonyl]-1,$N^6$-ethenoadenosine diphosphate (CBHεADP) and 2′-deoxy-3′-*O*-[[(phenylhydroxymethyl)phenyl]carbonyl]-1,$N^6$-ethenoadenosine diphosphate [3′(CBH)2′dεADP]. These derivatives were synthesized as fluorescent analogues of the expected product of the photochemical reactions of $Bz_2\epsilon$ADP and 3′($Bz_2$)2′dεADP, respectively, with the active site of $SF_1$. The fluorescence properties of the carboxybenzhydrol derivatives trapped at the active site by pPDM were compared with those of the $Bz_2$ nucleotide–$SF_1$ complexes. These properties were consistent with a photoincorporation mechanism in which the carbonyl of benzophenone was converted to a tertiary alcohol attached covalently to the protein. The specific, highly efficient photoincorporation of $Bz_2\epsilon$ADP at the active site will allow it to be used as a donor in distance measurements by fluorescence resonance energy transfer to acceptor sites on actin.

Myosin is the key enzyme involved in energy transduction in muscle contraction, utilizing the chemical energy released upon hydrolysis of ATP to generate mechanical force required for movement (Morales et al., 1982). In spite of extensive research on binding and hydrolysis of ATP by myosin, little is known about the conformational changes implied in the actomyosin adenosine triphosphatase (ATPase) mechanism. It is not known whether postulated ATP-dependent conformational changes involve global changes in myosin subfragment 1 ($SF_1$)[1] structure or whether structural changes occur only in the vicinity of the ATPase site. The heads of myosin are thought to be comma-shaped (Winkelmann et al., 1985) with the ATP binding site located about two-thirds the distance from the rod–neck junction to the distal end (Sutoh et al., 1985; Munson et al., 1985). The location of the actin binding site is less well-defined, but it is also believed to span the end one-third of the head (Vibert & Craig, 1982; Vibert et al., 1986).

The dimensions of the heads of myosin and of actin monomers (Botts et al., 1984) and the apparent proximity of the myosin ATP binding and actin binding sites mean that it should be possible, with appropriate probes, to measure the

†Supported by grants from the Muscular Dystrophy Association and NIH (DK 05195). The Varian 2200 spectrophotometer used in these studies was purchased with funds provided by NSF Equipment Grant PCM-8400841.

‡Postdoctoral fellow of the Muscular Dystrophy Association and the American Heart Association.

[1] Abbreviations: $SF_1$, myosin subfragment 1; εADP, 1,$N^6$-ethenoadenosine diphosphate; εAMP-PNP, 1,$N^6$-ethenoadenyl-5′-yl imidodiphosphate; DPH, 1,6-diphenyl-1,3,5-hexatriene; pPDM, *N*,*N*′-*p*-phenylenedimaleimide; HEPES, *N*-(2-hydroxyethyl)piperazine-*N*′-2-ethanesulfonic acid; $Bz_2\epsilon$ADP, 3′(2′)-*O*-(4-benzoylbenzoyl)etheno-adenosine 5′-diphosphate; $Bz_2$ADP, 3′(2′)-*O*-(4-benzoylbenzoyl)adenosine 5′-diphosphate; CBH, 4-carboxybenzhydrol; $Bz_2$, 4-benzoylbenzoyl; $Bz_2$ acid, 4-benzoylbenzoic acid; TLC, thin-layer chromatography; 2′dADP, 2′-deoxyadenosine 5′-diphosphate; CBHεADP, 3′(2′)-*O*-[[(phenylhydroxymethyl)phenyl]carbonyl]ethenoadenosine 5′-diphosphate; 3′-($Bz_2$)2′dεADP, 3′-*O*-(4-benzoylbenzoyl)-2′-deoxyethenoadenosine 5′-diphosphate; 3′(CBH)2′dεADP, 3′-*O*-[[(phenylhydroxymethyl)phenyl]-carbonyl]-2′-deoxyethenoadenosine 5′-diphosphate; FRET, fluorescence resonance energy transfer; DMF, dimethylformamide; HPLC, high-performance liquid chromatography; TEAB, triethylammonium bicarbonate; POPOP, 1,4-bis[2-(5-phenyloxazolyl)]benzene; Tris, tris(hydroxymethyl)aminomethane; MeOD, deuteriated methanol; EDTA, ethylenediaminetetraacetic acid; SDS–PAGE, sodium dodecyl sulfate–polyacrylamide gel electrophoresis.

0006-2960/87/0426-7524$01.50/0 

distance between myosin's active site and specific sites on actin by use of fluorescence resonance energy transfer (FRET). Many intramolecular measurements in both myosin and actin have been made by using this technique, but only a few intermolecular distances have been measured in actomyosin (Takashi, 1979; Trayer et al., 1982; Miki & Wahl, 1984) and the actin–myosin–nucleotide ternary complex (dos Remedios & Cooke, 1984; Trayer & Trayer, 1983; Bhandari et al., 1985). The only report, to our knowledge, of a distance measurement between the active site on $SF_1$ to sites on actin was by dos Remedios and Cooke (1984). These measurements were made with reversibly bound donors or acceptors at the active site on $SF_1$ in the presence of variously labeled actin preparations. This approach required high protein concentrations to form appreciable amounts of the ternary complex (Trayer & Trayer, 1983). The surface fluorescence from thin cells at 45 °C to the incident beam was measured to minimize the problems of high turbidity and absorbance that cause scattering and secondary reabsorption of the emission. Under these conditions, dos Remedios and Cooke (1984) estimated the distance from the myosin ATPase site to the F-actin nucleotide binding site and to Cys-374 of actin to be greater than 10 and ~6 nm, respectively.

The purpose of the present work was to repeat measurements of this type after attaching a fluorophore covalently by photoaffinity labeling the active site of myosin. This approach should allow lower protein concentrations to be used and should avoid the problems of resolving multiple fluorescent lifetimes inherent in ternary system studies. As a first step we have synthesized ADP photoaffinity analogues, e.g., $Bz_2\epsilon$ADP, that combine the well-characterized fluorescent properties of $\epsilon$ADP [for review, see Leonard (1984)] with the photolabeling capability of benzophenone (Galardy et al., 1973; Williams & Coleman, 1982). Our work was guided by the knowledge that the parent derivative, $Bz_2$ADP, can be trapped at the active site by thiol cross-linking agents and stably photoincorporated in 50–60% yields (Mahmood & Yount, 1984). High yields of photolabeling are essential in order to do subsequent fluorescence measurements at low protein concentrations. In addition, it was reasonable to expect that $Bz_2\epsilon$ADP and related derivatives would be stably trapped at the active site in a manner analogous to that of $Bz_2$ADP. Trapping, which allows unbound nucleotide to be removed before irradiation, has been found to be essential for specific active site photolabeling of myosin with a variety of photoprobes (Mahmood & Yount, 1984; Mahmood and Yount, unpublished results; Nakamaye et al., 1985; Grammer & Yount, 1985). Covalent attachment is essential to do active site to actin distance measurements because actin is known to destabilize nucleotides trapped at the active site by thiol cross-linking agents (Chalovich et al., 1983).

This paper describes the synthesis and characterization of four new derivatives of $\epsilon$ADP. Two of these derivatives, $Bz_2\epsilon$ADP and $3'(Bz_2)2'd\epsilon$ADP, specifically photoincorporate into the active site of $SF_1$. This is the first report of fluorescent photoaffinity labels for the myosin active site. The other two probes which contain reduced benzophenone moieties were used as spectral models of the irradiated enzyme–analogue complexes. We have characterized the steady-state and time-resolved fluorescence properties of the free nucleotides in solution, reversibly bound, and trapped at the active site and the covalent nucleotide–protein complexes in preparation for the intermolecular distance measurements discussed above. The fluorescent properties of $Bz_2\epsilon$ADP, covalently incorporated at the active site of $SF_1$, indicate that it will be useful as a donor in distance measurements by FRET to acceptor sites on actin and as a probe of actin-mediated structural changes sensed at the $SF_1$ active site.

## Materials and Methods

The sources of commercial compounds were as follows: sodium adenosine diphosphate (P-L Biochemicals), [2,8-$^3$H]ADP (New England Nuclear), trypsin, chymotrypsin, quinine sulfate, reagents for gel electrophoresis, carbonyldiimidazole, LH-20-100, and 2′dAMP (Sigma), benzoylbenzoic acid and pPDM (Aldrich), DPH (Molecular Probes), and POPOP (Eastman). $\epsilon$ADP and $2'd\epsilon$ADP were purified by DEAE chromatography by use of TEAB gradients after synthesis from ADP and 2′dADP by the method of Secrist et al. (1972). Solvents used in fluorescence measurements were spectrograde (Baker). $\epsilon$AMP-PNP was prepared from $\epsilon$AMP and imidodiphosphate by the coupling procedure of Hoard and Ott (1965). Analytical TLC plates (Analtech, silica gel GF) were run in solvent systems A, 1-butanol/$H_2O$/acetic acid (5:3:2), and B, isobutyric acid/ammonium hydroxide/water (75:1:24), at room temperature, and spots were visualized by UV light at 254 nm. Total phosphate was analyzed as described by Ames and Dubin (1960) using ATP and $K_2HPO_4$ as standards. DMF was dried by distillation from tosyl chloride.

ATPase assays were performed as described previously (Wells et al., 1979b), except that release of inorganic phosphate was measured at 2 and 8 min after the addition of $SF_1$ to the assay mixture. Protein concentrations were measured by the Coomassie blue dye binding method of Bradford (1976) with unmodified $SF_1$ as a standard as previously described (Wells et al., 1979a). Liquid scintillation counting was performed on a Beckman LS 7500 with aqueous counting scintillant (Amersham).

*Protein Preparation.* Rabbit skeletal myosin was prepared according to Wagner and Yount (1975) and was stored in 50% glycerol at −20 °C. Chymotryptic $SF_1$ was prepared as described by Weeds and Taylor (1975) and was assumed to have a molecular weight of 115000 and an $\epsilon_{280}^{1\%} = 7.5$ cm$^{-1}$ (Wagner & Weeds, 1977). $SF_1$ was stored at 0 °C and used within 2 weeks.

*Enzyme Modifications.* Nucleotides were trapped at the active site of $SF_1$ by pPDM as described by Wells and Yount (1982). Specific conditions are described in the figure legends. A pH 7.0 buffer (50 mM HEPES, 0.1 M KCl) was used throughout to minimize ester hydrolysis of the $Bz_2$ nucleotides. Inactivations, purification, and lifetime studies on a given sample were completed within 24 h. After quenching of the pPDM thiol cross-linking reaction with $\beta$-mercaptoethanol, the mixture was incubated for 10 min on ice in the presence of ATP (50-fold excess over $SF_1$) and EDTA (20 mM final concentration) to minimize nonspecific nucleotide binding. Excess thiol reagents, EDTA, and untrapped nucleotide were then removed by gel filtration on a 5-mL Sephadex G-50 fine column (equilibrated in KCl–HEPES buffer, pH 7.0) as described by Penefsky (1977). For photoincorporation studies, samples were irradiated within 30 min of purification to minimize the effects of slow nucleotide leakage from the active site (see Results and Discussion).

*Irradiation Procedure.* Solutions of pPDM-modified $SF_1$ containing trapped nucleotide analogue in KCl–HEPES buffer (pH 7.0) were continuously irradiated with an Ace-Hanovia 450-W medium-pressure quartz mercury vapor lamp at a distance of 9 cm. A 5-cm Pyrex Petri dish was suspended in a stirred ice bath and covered with a Pyrex plate to filter out radiation below 300 nm. The Pyrex plate was exchanged with

an ice-cold plate every 5 min. Under these conditions the protein solution remained ice cold and the $NH_4^+$-ATPase activity of an unmodified $SF_1$ sample was within 5% of an unphotolyzed control after 90-min photolysis.

*Tryptic Digestion of $SF_1$ and SDS–PAGE Analysis.* $SF_1$ was digested with 1/100 (w/w) trypsin in KCl–HEPES buffer (pH 7.0) at 25 °C for 30 min. The reaction was terminated by boiling 2 parts protein solution with 1 part concentrated sample buffer (Laemmli, 1970) for 2 min. The $SF_1$ fragments were separated on gels by using 12% acrylamide, 0.32% bisacrylamide, and 0.1% SDS. The gel was stained in 0.05% Coomassie blue in 45% methanol, 45% $H_2O$, and 10% glacial acetic acid and then destained by using the same solvent without the dye. The gels were sliced (1.5 mm) and solubilized by heating for 8 h at 75 °C in 0.75 mL of 30% $H_2O_2$–concentrated $NH_4OH$ solution (99:1). After cooling, 0.5 mL of 0.5 M acetic acid was added before counting in 10-mL aqueous scintillant.

*Steady-state fluorescence measurements* were made with an SLM 4800 fluorometer (SLM Instruments, Urbana, IL), which was interfaced with an HP 9825A computer and HP 7225A plotter. Corrected emission spectra were made with the excitation polarizer (Glan-Thompson) at 55° from vertical and the emission polarizer at 0°. All slits were adjusted to a 4-nm band-pass. Correction factors were obtained by calibrating the emission monochromator and photomultiplier with a standard tungsten light source. Intensity fluctuations of the xenon lamp and variations in the efficiency of the excitation monochromator were corrected by using a Rhodamine B quantum counter in the reference detector. Water Raman and $SF_1$ scattering intensity were subtracted from emission spectra where appropriate. All solutions were filtered through a Millex-PF 0.8-$\mu$m filter to minimize light scattering.

Fluorescence quantum yields were determined relative to quinine sulfate in 0.1 N $H_2SO_4$ by using the relationship of Parker and Reese (1960). A Varian 2200 spectrophotometer was used to measure absorbance in 3-mL cuvettes. Samples were diluted to an absorbance of <0.02 for fluorescence measurements.

*Fluorescence lifetime measurements* were made with the SLM 4800 fluorometer. Band-pass settings were 8 nm prior to the excitation monochrometer, 0.5 nm prior to the modulation tank, and 0.5 nm prior to the sample. The emission band-pass was set at 16 nm. Alternatively, for low-intensity samples, the emission monochrometer was bypassed and replaced with a 389-nm cutoff filter. To eliminate the effects of anisotropic rotation on fluorescence lifetimes, the Glan-Thompson excitation polarizer was set at 35° from vertical, and the emission was observed without a polarizer (Spencer & Weber, 1970).

Lifetimes were determined by the phase shift and demodulation of fluorescence of a sample relative to a standard reference compound (Lakowicz et al., 1980, 1981; Dalbey et al., 1984). The reference compounds were POPOP and DPH, which have lifetimes of 1.3 and 8.7 ns, dissolved in air-equilibrated absolute ethanol and cyclohexane, respectively, at 6 °C. Standard lifetimes were measured at $\lambda_{ex}$ = 320 or 330 nm and $\lambda_{em}$ = 410 nm, which were the same settings used to measure ethenonucleotide lifetimes. The Debye–Sears acoustooptical modulation tank was tuned as described by Dalbey et al. (1984), using POPOP as the primary standard. DPH was used as the reference compound for ethenoadenosine nucleotide lifetime measurements.

Data were acquired with an HP 9825A computer. One set of data was the average of 15 values of the phase- and modulation-derived lifetimes, $\tau_p$ and $\tau_m$, at each of the three modulation frequencies (6, 18, and 30 MHz). Three data sets were routinely collected for each sample on a given day. The average of these three data sets represented a single phase and modulation measurement. This measurement was then repeated $n$ times on different days to provide the input data for the heterogeneity analysis described below. The nonlinear least-squares method described by Lakowicz et al. (1984) was used to determine the lifetimes ($\tau_i$) and fractional intensities ($f_i$) for a mixture of exponentially decaying fluorophores. A Marquardt algorithm was used to estimate $f_i$ and $\tau_i$ to minimize $\chi_R^2$, the error-weighted sum of the squared deviations between the measured and calculated values of the phase and modulation at each frequency ($\omega$) divided by the number of degrees of freedom.

We assume that the estimated errors in the phase and modulation data are frequency independent and are set to 0.2° and 0.004, respectively. These values are within the range estimated by Gratton et al. (1984) in the 6–30-MHz region for their instrument but may underestimate the average random errors of our instrument. Values of $\chi_R^2$ (Table II) consistently greater than 1 may reflect this underestimate. The uncertainties in $\tau_i$ and $f_i$ may also be underestimated, but the relative magnitudes are still a useful measure of uncertainty between similar sets of measurements.

*Syntheses.* $Bz_2\epsilon$ADP and [$^3$H]$Bz_2\epsilon$ADP were synthesized from $\epsilon$ADP (sodium salt) or [2,8-$^3$H]$\epsilon$ADP and 4-benzoylbenzoic acid by the method of Gottikh et al. (1970). [$^{14}$C]-$Bz_2\epsilon$ADP was synthesized in a similar manner from $\epsilon$ADP and [1-$^{14}$C-*carboxy*]-4-benzoylbenzoic acid (Nakamaye & Yount, 1985). In a typical synthesis, $Bz_2$ acid (0.25 mmol) and carbonyldiimidazole (0.85 mmol) were stirred for 15 min at room temperature in 0.32 mL of dry DMF. $\epsilon$ADP (0.1 mmol) was dissolved in 0.625 mL of $H_2O$ and added dropwise to the reaction. Acetonitrile (0.625 mL) was then added to yield a clear mixture which was stirred at room temperature for 12–16 h. After rotoevaporation to dryness the unreacted $Bz_2$ acid was removed by repeated acetone washes followed by centrifugation. The dried powder was dissolved in 2 mL of 0.1 M NaCl, and this solution was loaded onto a 2.2 × 100 cm Sephadex LH-20-100 column equilibrated in $H_2O$ at 4 °C. The flow rate was 0.5 mL/min, and 2.5-mL fractions were collected. Unreacted $\epsilon$ADP and $Bz_2\epsilon$ADP eluted at ~40% and ~80% respectively, of the total bed volume as measured by absorbance at 260 nm. A small amount of UV absorbance was detected in an unknown broad peak which eluted between the above peaks. Residual $Bz_2$ acid eluted immediately after the desired products; thus, the thorough acetone washing step prior to column chromatography was essential to avoid cross contamination of the products with $Bz_2$ acid. The products migrated as two poorly resolved nonfluorescent spots at $R_f$ 0.34 and 0.36 (solvent A) and $R_f$ 0.49 and 0.51 (solvent B) on TLC and were presumed to represent the presence of both 2′ and 3′ isomers (see Results and Discussion). Contaminating $\epsilon$ADP ($R_f$ 0.15, solvent A) or $Bz_2$ acid ($R_f$ 0.9, solvent A) was not detected (<1%) by TLC. HPLC analysis (Mahoney & Yount, 1984) showed a single but broad peak eluting later than $\epsilon$ADP or $Bz_2$ acid standards. The average yield = 20 ± 5% in four syntheses. The product pool was adjusted to pH 5.0 and stored at −80 °C in small aliquots to minimize ester hydrolysis.

$^1$H NMR ($D_2O$, pH ~5.0) $\delta$ 8.94 (s, 1 H, $C_2$), 8.59 (s, 0.63 H, $C_8$, 3′ isomer), 8.52 (s, 0.38 H, $C_8$, 2′ isomer), 8.1–7.3 (m, 11.7 H, phenyl rings + etheno ring), 6.42 (d, 0.38 H, $C_{1'}$, 2′ isomer), 6.26 (d, 0.63 H, $C_{1'}$, 3′ isomer), 5.79 (dd, 0.40 H, $C_{2'}$, 2′ isomer), 5.72 (dd, 0.60 H, $C_{3'}$, 3′ isomer), 5.13 (dd, 0.60

H, $C_{2'}$, 3′ isomer), 4.5 (br, 0.63 H, $C_{4'}$, 3′ isomer), 4.38 (br, 0.38 H, $C_{4'}$, 2′ isomer), 4.21 (br, 2.0 H, $C_{5'}$); 2′ isomer of $C_{3'}$ under $H_2O$ peak. NMR spectra were measured on a Nicolet 200-MHz spectrometer at 4 °C. Proton assignments were based upon coupling constants and the results of homodecoupling experiments.

CBHεADP was synthesized from εADP and CBH exactly as described for $Bz_2$εADP. The products migrated as two poorly resolved fluorescent spots at $R_f$ 0.44 and 0.46 (solvent B). CBH was synthesized from $Bz_2$ acid by modifying the synthesis of benzhydrol from benzophenone by zinc reduction in base (Gilman & Blatt, 1941), where the volume of 95% EtOH was increased 10-fold and enough water was added to dissolve the sodium salt of $Bz_2$ acid. CBH was crystallized from 95% EtOH, washed with cold $H_2O$, and recrystallized from hot $H_2O$ before drying over $P_2O_5$. Anal. (M.W.H. Laboratories, Phoenix, AZ) Calcd for CBH: C, 73.7; H, 5.3; O, 21.0. Found: C, 73.67; H, 5.25; O, 21.03; mp 155–156 °C (lit. mp 164–165 °C; Zincke, 1872). For the potassium salt of CBH, $\epsilon^{M}_{236}$ = 15 500 L/(mol·cm) in KCl–HEPES buffer, pH 7, as determined gravimetrically. The $^1$H NMR of CBH in MeOD confirmed the presence of 10 phenyl protons with a singlet at 5.8 corresponding to the aliphatic proton. CBH was free (<1%) of unreacted $Bz_2$ acid as determined by comparing the $^1$H NMR data for both CBH and $Bz_2$ acid.

3′($Bz_2$)2′dεADP and 3′([$^{14}$C]$Bz_2$)2′dεADP were synthesized from the tributylammonium salt of 2′dεADP and $Bz_2$ acid or [1-$^{14}$C-*carboxy*]-4-benzoylbenzoic acid, respectively. Carbonyldiimidazole (0.5 mmol) and $Bz_2$ acid (0.25 mmol) were dissolved in 0.5 mL of dry DMF and stirred for 15 min at room temperature under an argon purge. Excess carbonyldiimidazole was quenched with 0.5 mmol of MeOH (0.02 mL) before slowly adding a mixture of 0.1 mmol of tributylamine and 0.05 mmol of 2′dεADP in 0.25 mL of DMF. This addition yields a slightly cloudy reaction mixture. The presence of tributylamine was essential at this step. Without tributylamine the nucleotides precipitated, presumably as the imidazolium salts, and no product was obtained. The reaction was stirred overnight at room temperature under a stream of argon which removed nearly all the DMF. Water was added and the insoluble $Bz_2$ acid removed by centrifugation. The supernatant containing 3′($Bz_2$)2′dεADP was removed and the $Bz_2$ acid pellet dissolved in acetone. The solution was centrifuged to pellet the residual 3′($Bz_2$)2′dεADP which was caught in the original $Bz_2$ acid precipitate. This precipitate and 3′($Bz_2$)-2′dεADP in solution were combined, brought to 0.1 M NaCl in $H_2O$, and purified exactly as described for $Bz_2$εADP. 3′-($Bz_2$)2′dεADP showed a single nonfluorescent spot at $R_f$ 0.37 (solvent A) and 0.51 (solvent B). Yield = 30% in two syntheses.

3′(CBH)2′dεADP was synthesized exactly as described for 3′($Bz_2$)2′dεADP except that the nucleotides from the reaction mixture were precipitated as the sodium salts from DMF and acetone by adding NaI dissolved in acetone and then washing with acetone before LH-20 chromatography as described in the $Bz_2$εADP synthesis. $\epsilon^{M}_{275}$ = 11 400 ± 1000. 3′(CBH)-2′dεADP migrated as a single fluorescent spot at $R_f$ 0.38 (solvent A) and 0.52 (solvent B).

## Results and Discussion

*Synthesis and Chemical Characterization of Nucleotide Analogues.* The UV spectra of $Bz_2$εADP and CBHεADP are shown in Figure 1. The peak at 264 nm and shoulder at 275 nm for $Bz_2$εADP are consistent with the presence of the $Bz_2$ group [$\epsilon^{M}_{264}$ of 4′-benzoylbenzoate = 20 000 L/(mol·cm)] and the etheno modification of the adenine ring [$\epsilon^{M}_{265}$ = 5700 L/(mol·cm) and $\epsilon^{M}_{275}$ = 5600 L/(mol·cm); Secrist et al., 1972], respectively. $\epsilon^{M}_{264}$ was 32 250 ± 1500 L/(mol·cm), on the basis of total and acid-labile phosphate analyses. The UV spectrum and molar extinction coefficient of 3′($Bz_2$)2′dεADP were identical with those for $Bz_2$εADP. These extinction coefficients were independently verified from the specific activities of the tritiated and carbon-14-labeled derivatives. The major peak at 230 nm (CBH) and the minor peak at 275 nm (etheno-adenosine) were consistent with the proposed CBHεADP structure (Figure 1). $\epsilon^{M}_{230}$ was 53 400 ± 3000 on the basis of total and acid-labile phosphate analyses. The shape of the UV spectrum of 3′(CBH)2′dεADP was similar to that for CBHεADP except that the peak at 230 nm was 10 ± 1% lower. $\epsilon^{M}_{230}$ = 48 000 ± 2000, and $\epsilon^{M}_{275}$ = 11 400 ± 700, on the basis of total and acid-labile phosphate analyses.

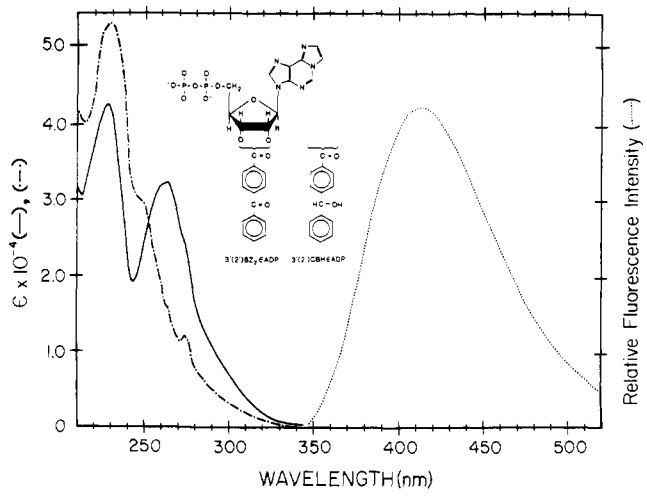


FIGURE 1: Fluorescence emission (···) spectrum of $Bz_2$εADP and UV absorption spectra of $Bz_2$εADP (—) and CBHεADP (-·-). The fluorescence emission spectrum was corrected as described under Materials and Methods with the excitation and emission polarizers at 55° and 0° from the vertical. $\lambda_{ex}$ = 330, $T$ = 6 °C. The excitation and emission band-pass settings were 4 nm. All spectra were taken in HEPES–KCl buffer, pH 7.0.

The $^1$H NMR spectrum (see Materials and Methods) for $Bz_2$εADP was consistent with the proposed structure (Figure 1). The total peak integrations attributed to the $Bz_2$ protons and the adenosine protons were consistent with one $Bz_2$ group per adenosine. The results rule out the presence of a possible 2′,3′-disubstituted compound. The structure for $Bz_2$εADP shown in Figure 1 indicates that the product is a mixture of isomers, esterified at either the 2′ or 3′ hydroxyl of the ribose. $^1$H NMR was used to assay the proportions of the 2′ and 3′ isomers by measuring the relative peak areas of the resonance signals $H_8$, $H_{1'}$, $H_{2'}$, and $H_{3'}$ for the two isomers. This method has been used to measure rates of hydrolysis and acyl migration of ribonucleoside derivatives (Griffin et al., 1966). The $^1$H NMR results indicate that $Bz_2$εADP (and CBHεADP, data not shown) is a mixture of 3′- and 2′-monosubstituted isomers in a ratio of 60/40. Griffin et al. (1966) have shown that the rate of equilibration of 3′-*O*-acetyluridine to a mixture of the 2′ and 3′ isomers is very rapid ($t_{1/2}$ = 1 min at pH 7.0). Therefore, it is likely that acyl migration had reached equilibrium before the pH was lowered to 5 for the $^1$H NMR measurement of $Bz_2$εADP.

These results are in agreement with those of McLaughlin and Ingram (1965a,b) who found a 3′/2′ ratio of 65/35 for (aminoacyl)adenosine using a chemical method and a 75/25 ratio for (*N*-acetylvalyl)adenosine using a chromatographic approach. These reports are in contrast to those of Williams and Coleman (1982) and Kambouris and Hammes (1985) who

indicated that their preparations of $Bz_2ATP$ contained only the 3′ isomer on the basis of $^1H$ NMR results. However, the $^1H$ NMR analysis of $Bz_2ATP$ prepared by their method (Mahmood and Yount, unpublished results) indicated a 3′/2′ isomeric ratio of 60/40, identical with the results presented here for $Bz_2\epsilon ADP$. Abeijon et al. (1986) concluded that their preparation of $Bz_2CTP$ was also only the 3′ isomer, on the basis of $^1H$ NMR results. A reason for these discrepancies may be the pH dependence of the $^1H$ NMR spectrum of *O*-acyl nucleotides. The rate of acyl migration at higher pH values will broaden the signals from the ribose protons (Griffin et al., 1966). At pH 7 we have found considerable signal broadening that prevented definitive assignments of the 2′ and 3′ isomer signals. Guillory and Jeng (1977) have interpreted their $^1H$ NMR spectrum of (arylazido)-β-alanyl-ATP as only the 3′ isomer. However, depending upon the pH of the sample (not reported) the reported chemical shifts and signals may represent the combined broadened signals of the 2′ and 3′ isomers.

The nucleotide purification method described here, using Sephadex LH-20 eluted with $H_2O$, is modified from the general method described by Hiratsuka (1983). In our hands, this method was more reproducible than LH-20 eluted with ammonium formate as described by Williams and Coleman (1982) and easier than DEAE-Sephadex eluted with TEAB (Mahmood et al., unpublished results). If LH-20 is eluted with water, the salt concentration of the sample load must be ~0.1 M; without the salt present $\epsilon ADP$ and $Bz_2\epsilon ADP$ did not resolve. The column was recycled by washing with water in situ and did not retain benzoylbenzoate. No lyophilization was necessary as the products emerged as a sharp peak in a concentration range (0.5–2.0 mM) appropriate for most experiments. Our lifetime experiments were very sensitive to the presence of hydrolyzed product because of the markedly higher quantum yield of $\epsilon ADP$ vs $Bz_2\epsilon ADP$ (see Table I). $Bz_2\epsilon ADP$ purified by the method of Williams and Coleman (1982) from two syntheses contained 5–7% $\epsilon ADP$ as measured by the fractional fluorescence intensity of the contaminating $\epsilon ADP$ lifetime. By the method described here, however, the product appeared to be homogeneous, indicating <0.3% $\epsilon ADP$ contamination. In general, we have not detected hydrolysis of purified samples stored for up to 6 months at −80 °C in water, pH 5.0. However, $Bz_2\epsilon ADP$ stored at 4 °C for 2 weeks (pH 7.0) showed 5.5% contamination due to hydrolysis to $\epsilon ADP$ and $Bz_2$ acid as measured by fluorescence lifetimes.

*Inactivation of $SF_1$ and Trapping of Ethenonucleotides in the Presence of pPDM.* Wells and Yount (1979) have shown that treating $SF_1$ with various thiol cross-linkers in the presence of excess MgADP cross-links SH1 and SH2 and traps MgADP, as a 1:1 complex, stably and noncovalently at the active site. A linear correlation between the loss of ATPase activity and the stoichiometry of trapped nucleotide has been demonstrated for a variety of cross-linking reagents (Wells et al., 1980). The rate of inactivation of $SF_1$ ATPase by various thiol cross-linking reagents was enhanced in the presence of Mg nucleotides (Wells et al., 1980).

The time course of inactivation of $SF_1$ CaATPase by pPDM in the presence and absence of ethenoadenosine derivatives is shown in Figure 2. Without nucleotide, the intramolecular cross-linking of SH1 and SH2 was slow enough to observe a transient stimulation of the CaATPase followed by a slow inactivation. The basis of this behavior has been described by Wells and Yount (1982) and by Reisler (1982). The rate of inactivation was enhanced in the presence of all nucleotides tested, suggesting modification of SH2. $Bz_2\epsilon ADP$ and 3′-$(Bz_2)$2′d$\epsilon ADP$ both exhibited slower rates of inactivation than

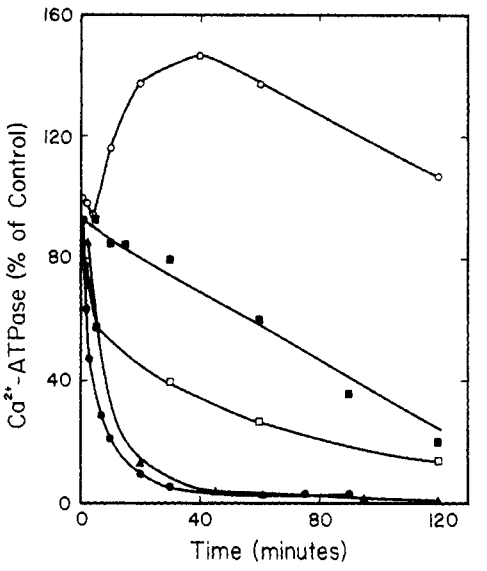


FIGURE 2: Inactivation of $SF_1$ CaATPase by pPDM in the presence and absence of ethenonucleotide derivatives. $SF_1$ (2.0 mg/mL; 17 μM) in HEPES–KCl buffer (pH 7.0) was equilibrated for 5 min with 34 μM nucleotide in the presence of 0.2 mM $MgCl_2$ at 0 °C. The inactivation was begun by adding a 1.2-fold excess (over enzyme) pPDM to each reaction. At indicated times, aliquots were removed and quenched with a 200-fold excess of β-mercaptoethanol before assaying for CaATPase activity. All values are expressed as percent of a control to which β-mercaptoethanol was added before adding pPDM. ○, no added nucleotide; ▲, $Bz_2\epsilon ADP$; ■, 3′$(Bz_2)$2′d$\epsilon ADP$; ●, ADP; □, 2′d$\epsilon ADP$.

their respective parent nucleotides, ADP and 2′dADP. Similar results were obtained for CBH$\epsilon ADP$ and 3′(CBH)2′d$\epsilon ADP$ (data not shown). This result may reflect a decreased reactivity of $SH_2$ in the presence of etheno nucleotides relative to the parent nucleotides as was suggested by the alkylation studies of Burke (1980). After 2-h incubation with pPDM, the residual CaATPase activity of both 2′-deoxy derivatives was greater (~20%) than for the 2′-OH nucleotides (~1–5%). The relative rates of $NH_4^+$-EDTA ATPase inactivation (data not shown) in the presence of these nucleotides were similar to the CaATPase data shown in Figure 2. In general, patterns of inactivations were similar to those seen by other workers using ATP and pPDM (Burke & Reisler, 1977; Wells & Yount, 1979) and with $Bz_2ATP$ and cobalt(III) phenanthroline (Mahmood & Yount, 1984).

*Equilibrium Binding of $Bz_2\epsilon ADP$ to $SF_1$.* The variation in polarization of $Bz_2\epsilon ADP$ as a function of the free $Bz_2\epsilon ADP$ concentration is shown in Figure 3. The apparent equilibrium dissociation constant calculated from the Scatchard analysis (Scatchard, 1949) was 5.5 μM, with a binding stoichiometry of 1.04. This result was consistent with $Bz_2\epsilon ADP$ interacting with a single class of sites on $SF_1$. The dissociation constant for $Bz_2\epsilon ADP$ was also measured by equilibrium dialysis under the same conditions (data not shown). The results of this Scatchard analysis were also consistent with a single binding site ($n = 1.0 \pm 0.08$) with a dissociation constant of 5.6 ± 0.5 μM. Mahmood and Yount (unpublished results) measured a dissociation constant of 3 μM ($n = 1.04$) for $Bz_2ATP$ by the same method, indicating that the etheno modification does not significantly alter the apparent dissociation constant.

*Molecular Fluorescence Emission.* The molecular fluorescence emission spectrum of $Bz_2\epsilon ADP$ in aqueous buffer at pH 7.0 forms a single unresolved band with a maximum at ca. 415 nm (Figure 1). The shape and position of this spectrum were identical with those of the spectrum of aqueous-buffered ε-adenosine hydrochloride (Secrist et al., 1972).[2]

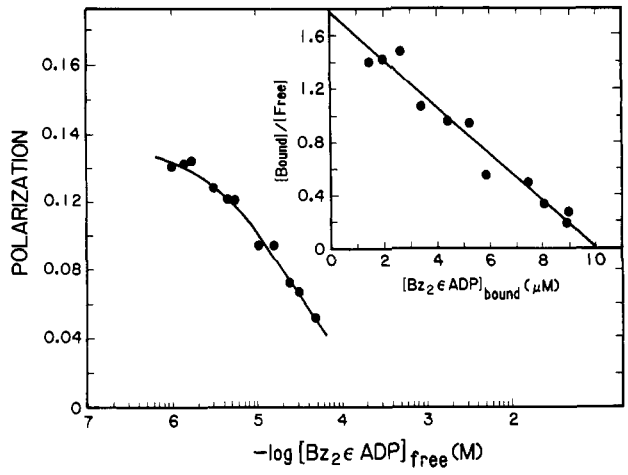


FIGURE 3: $Bz_2\epsilon ADP$ equilibrium binding to $SF_1$ measured by emission polarization. $SF_1$ was 10.5 $\mu$M in HEPES–KCl buffer, pH 7.0 at 6 °C. The excitation wavelength was 330 nm. Emission was detected without a monochrometer through a 408-nm cutoff filter. The excitation slits were as described for lifetime measurements to minimize photolysis of the probe during the experiment. Polarization values ($P$) at each added ligand concentration were corrected by subtracting the intensity of a 10.5 $\mu$M $SF_1$ blank at each polarizer setting. Data points were the average of triplicate measurements from two independent experiments. The limiting polarization of $Bz_2\epsilon ADP$ bound to $SF_1$ ($P_b$) was 0.219 (measured at 8.4 $\mu$M $Bz_2\epsilon ADP$, 169 $\mu$M $SF_1$). The polarization of free probe ($P_f$) was 0.019. The ratio of bound ($S$) to free ligand (1 − S) at each concentration of added ligand was determined by using the Weber (1952) equation below as modified by Rajkowski and Cittanova (1981). $I_f/I_b$ was from Table I, where

$$\frac{S}{1-S} = \frac{I_f(3-P_b)(P-P_f)}{I_b(3-P_f)(P_b-P)}$$

$I_f$ and $I_b$ were the quantum yields of the free and bound ligand, respectively. A nonweighted linear least-squares fit to a Scatchard plot of the data (see inset) gave a dissociation constant of 5.6 $\mu$M and a total site concentration of 10.0 $\mu$M. The curve drawn through the polarization data points was calculated from the law of mass action assuming a single class of sites and the above-calculated dissociation constant.

Identical blue Stokes shifts of ca. 6–7 nm were seen for $\epsilon$ADP, 2′d$\epsilon$ADP, $Bz_2\epsilon ADP$, 3′($Bz_2$)2′d$\epsilon$ADP, and the respective CBH derivatives upon binding to $SF_1$. As was observed by Perkins et al. (1984) for $\epsilon$ADP, no further blue shift was seen upon trapping these nucleotides at the active site with pPDM. Apparently, the bulky $Bz_2$ and CBH groups do not measurably affect the coplanarity of the purine ring in the protein binding site (Secrist et al., 1972). Secrist et al. (1972) reported that a blue Stokes shift in ethenoadenosine was mediated by an increase in solvent viscosity and reflected a restriction to changes in nuclear configuration involving bond angles in the purine ring. Therefore, the magnitude of this blue Stokes shift upon binding of the $\epsilon$-adenine ring to a protein, in general, can be a measure of the constraints imparted upon the purine ring by the binding site.

*Quantum Yields and Lifetimes of Ethenonucleotides Free in Buffer.* The results in Table I show the quantum yields of $\epsilon$ADP and $Bz_2$ derivatives free in buffer at 6 °C. The quantum yield of 0.75 ± 0.04 for $\epsilon$ADP at 6 °C was higher than the value of 0.56–0.59 measured by Secrist et al. (1972) at room temperature. This discrepancy was consistent with the temperature dependence of the quantum yield observed by Secrist et al. (1972); vibrational excitation may facilitate internal conversion competitive with fluorescence emission.

The quantum yield for both $Bz_2$ probes free in buffer were lower than for the parent fluorophore, $\epsilon$ADP (Table I). The quantum yields of $\epsilon$ADP in the presence and absence of an equimolar concentration of benzoylbenzoate were the same, indicating the absence of a trivial inner filter effect. The quantum yields of $Bz_2\epsilon ADP$ and 3′($Bz_2$)2′d$\epsilon$ADP differ significantly. $Bz_2\epsilon ADP$ has been shown by $^1H$ NMR (see Materials and Methods) to be a mixture of isomers (60% 3′-O and 40% 2′-O). Thus, the nearly 50% lower quantum yield of $Bz_2\epsilon ADP$ relative to 3′($Bz_2$)2′d$\epsilon$ADP may reflect a lower fluorescence emission from the 2′ isomer. Replacing the OH at the 2′ position of the ribose ring with a hydrogen does not modify the emission properties of $\epsilon$ADP as can be seen by the identical quantum yields of 2′d$\epsilon$ADP and $\epsilon$ADP (Table I). Assuming additive quantum yields of the 2′ and 3′ isomers of $Bz_2\epsilon ADP$ and that the quantum yield of the 3′ isomer equals the measured value for 3′($Bz_2$)2′d$\epsilon$ADP, then by fractional addition, the emission of 3′(2′)$Bz_2\epsilon ADP$ could be due to only the 3′ isomer.

Intramolecular quenching of the ethenoadenosine fluorescence by the $Bz_2$ groups could occur by both dynamic and static nondipolar mechanisms, or by dipolar FRET. Corey–Pauling–Koltun molecular models were used to compare possible conformations of the 2′ and 3′ isomers of the $Bz_2$ derivatives. A conformation in which the two ring systems are folded up or stacked upon one another was most readily assumed by the 2′ isomer. The ketone chromophore of benzophenone has an $n \rightarrow \pi^*$ transition near 350 nm with an extinction coefficient of 100–200 L/(mol·cm) (Figure 1; Turro, 1978). Considering that the range of distances from this chromophore to the ethenoadenine ring is <1.0 nm, the spectral overlap between the emission of the ethenoadenine ring and the absorption of the carbonyl may allow for intramolecular energy transfer. As an example, Haugland et al. (1969), in a study of the dependence of the kinetics of FRET on spectral overlap, used a ketone as the acceptor and *N*-methylindole as a donor. The donor and acceptor were fused in a rigid steroid that separated them by 1.02 nm. In our case, a quantitative analysis of the transfer efficiency to this nonfluorescent acceptor is complicated by possible nondipolar quenching mechanisms as discussed above. Static and dynamic mobility must also be considered, where the distance between the donor and acceptor may change during the lifetime of the donor. In this case, exponential fluorescence decay would not be predicted (Lakowicz, 1983).

The quenching of the ethenoadenine ring fluorescence by the $Bz_2$ group was also reflected in the lifetime measurements (see Table II). The lifetime of $Bz_2\epsilon ADP$ free in buffer was reproducibly shorter than that of the 2′-deoxy derivative (5.1 vs 6.1 ns). The $\chi_R^2$ for the fit to exponential decay for $Bz_2\epsilon ADP$ was always greater than for 3′($Bz_2$)2′d$\epsilon$ADP. This may be due to nonexponential decay or to multiple lifetimes that are too close together to be resolved by our method. A shorter mean lifetime for $Bz_2\epsilon ADP$ relative to 3′($Bz_2$)2′d$\epsilon$ADP was consistent with the quantum yield results (Table I). However, the ratio of the quantum yields for $Bz_2\epsilon ADP$ and 3′($Bz_2$)2′d$\epsilon$ADP (0.53) was lower than the ratio of the respective lifetimes (0.84), consistent with the presence of a statically quenched 2′ isomer.

The fluorescence properties of the CBH derivatives, CBH$\epsilon$ADP and 3′(CBH)2′d$\epsilon$ADP, were examined to determine the importance of the benzophenone carbonyl to the quenching of the ethenoadenine fluorescence. In the CBH compounds the carbonyl has been reduced to an alcohol

[2] The technical spectrum published by Perkins et al. (1984) had a maximum at 406 nm. The corrected molecular emission maximum was 415 nm, which was blue shifted to 408 nm upon binding to $SF_1$.

Table I: Quantum Yields of Ethenonucleotides at 6 °C[a]

| analogue | buffer[b] | n[c] | bound to $SF_1$[d] | n | trapped on $SF_1$[e] | n | irradiated[f] | n |
|---|---|---|---|---|---|---|---|---|
| ϵADP | 0.75 (0.04) | 7 | 0.60 (0.02) | 4 | 0.62 (0.02) | 3 | 0.61 | 1 |
| 2′dϵADP | 0.75 (0.10) | 3 | 0.57 (0.02) | 2 | 0.58 (0.04) | 2 | | |
| 3′($Bz_2$)2′dϵADP | 0.10 (0.01) | 5 | 0.13 (0.05) | 4 | 0.12 (0.04) | 4 | 0.23 (0.03) | 2 |
| $Bz_2$ϵADP | 0.053 (0.003) | 3 | 0.054 (0.011) | 4 | 0.021 (0.003) | 3 | 0.17 (0.02) | 3 |
| 3′(CBH)2′dϵADP | 0.71 (0.01) | 2 | 0.51 (0.04) | 4 | 0.36 (0.02) | 2 | | |
| CBHϵADP | 0.46 (0.01) | 2 | 0.38 (0.04) | 3 | 0.36 (0.07) | 3 | | |

[a] Quinine sulfate in 0.1 N $H_2SO_4$ was used as a standard; quantum yield, 0.735 (6 °C), 0.70 (25 °C). [b] HEPES–KCl buffer, pH 7.0. [c] Each quantum yield is the average of $n$ experiments with the standard deviation given in parentheses. For $n = 2$, the range is given in parentheses. [d] Under conditions where >90% of nucleotide is bound to $SF_1$. The $SF_1$ concentrations ranged from 150 to 180 μM, and the nucleotide concentrations were from 5 to 12 μM. [e] Trapped and purified as described under Materials and Methods. [f] Irradiated as described under Materials and Methods for 60 (ϵADP), 50 ($Bz_2$ϵADP), and 80 min [3′($Bz_2$)2dϵADP].

Table II: Fluorescence Lifetimes of ϵADP Analogues[a]

| sample | lifetimes $\tau_i$ (ns) | fractional fluorescence $f_i$ | $\chi_R^2$ |
|---|---|---|---|
| ϵADP | | | |
| buffer[b] | 26.5 (0.3)[d] | 1.0 | 1.6 |
| trapped or bound[b,c] | 20.6 (0.4) | 0.91 (0.02) | 3.2 |
| | 2.7 (1.0) | 0.09 (0.02) | |
| $Bz_2$ϵADP | | | |
| buffer | 5.1 (0.3) | 1.0 | 30 |
| bound[c] | 12 (2) | 0.7 (0.1) | 5.0 |
| | 3.0 (0.5) | 0.3 (0.1) | |
| trapped | 11.6 (0.4) | 0.67 (0.02) | 2.0 |
| | 1.8 (0.2) | 0.33 (0.02) | |
| irradiated | 21.2 (0.4) | 0.90 (0.02) | 1.9 |
| | 5.5 (0.7) | 0.10 (0.02) | |
| 3′($Bz_2$)2′dϵADP | | | |
| buffer | 6.1 (0.2) | 1.0 | 7.3 |
| bound[c] | 9.9 (0.6) | 0.80 (0.09) | 3.2 |
| | 3.5 (1.1) | 0.20 (0.09) | |
| trapped | 11.4 (0.7) | 0.70 (0.07) | 2.8 |
| | 4.0 (0.5) | 0.30 (0.07) | |
| CBHϵADP | | | |
| buffer | 25.6 (0.2) | 0.90 (0.004) | 3.0 |
| | 4.2 (0.2) | 0.10 (0.004) | |
| bound[c] or trapped | 19.9 (1.7 | 0.80 (0.1) | 2.8 |
| | 8.7 (1.0) | 0.20 (0.1) | |
| 3′(CBH)2′dϵADP | | | |
| buffer | 24.7 (0.3) | 0.98 (0.02) | 2.0 |
| | 6.7 (1.1) | 0.02 (0.02) | |

[a] Analyses were performed at 6 °C in 100 mM KCl and 50 mM HEPES, pH 7.0. [b] Perkins and Yount, unpublished results. [c] Under conditions where >90% of added nucleotide is bound to $SF_1$ as described in Table I. [d] Values within parentheses were uncertainties in $\tau_i$ or $f_i$ as described under Materials and Methods.

(Figure 1) and can no longer serve as an energy-transfer acceptor of the ethenoadenine fluorescence. In this study, we used the CBH etheno derivatives as spectral models of the covalent adduct expected from the photoincorporation reaction of the $Bz_2$ ethenoadenosine probes with $SF_1$ (Figure 4; for discussion see Photoincorporation of pPDM-Trapped Ethenonucleotide Derivatives into $SF_1$).

The quantum yields and lifetimes of CBH derivatives free in solution were higher than those of the respective $Bz_2$ probes (Tables I and II). This result can be explained by the absence of quenching by intramolecular energy transfer for the CBH compounds, as discussed above. Again, as was seen for the $Bz_2$ compounds, there was a significant difference between CBHϵADP and 3′(CBH)2′dϵADP in both lifetimes and quantum yields. CBHϵADP, with 40% contribution from the 2′ isomer, has a lower quantum yield (0.46) than 3′(CBH)-2′dϵADP (0.71). The quantum yield of 3′(CBH)2′dϵADP was not significantly different from that of ϵADP. Assuming additive quantum yields of the 2′(3′) isomers in CBHϵADP and that the quantum yield of the 3′ isomer equals the measured value for 3′(CBH)2′dϵADP, then by fractional addition, nearly all of the fluorescence was due to the 3′ isomer. This analysis indicates that only the CBH in the 2′ position on the ribose ring quenched the ethenoadenine fluorescence.

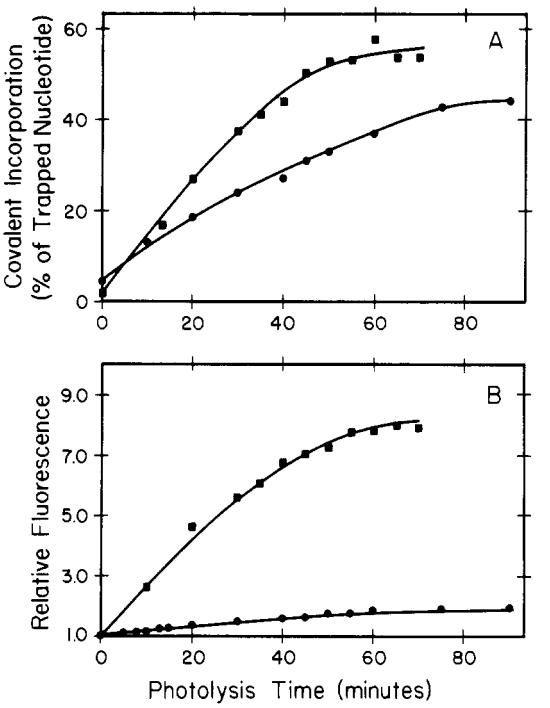


FIGURE 4: Time course of photoincorporation of [$^{14}$C]$Bz_2$ϵADP (■) and 3′([$^{14}$C]$Bz_2$)2′dϵADP (●) trapped on $SF_1$ by pPDM. $SF_1$ (30.4 μM) was inactivated in the presence of pPDM and nucleotide analogue for 2 h as described in Figure 2. After purification by gel filtration (see Materials and Methods), trapping was determined to be 0.70 ± 0.04 and 0.57 ± 0.03 mol of nucleotide/mol of $SF_1$ for [$^{14}$C]-$Bz_2$ϵADP and 3′([$^{14}$C]$Bz_2$)2′dϵADP, respectively. The specific activity of both analogues was 5400 cpm/nmol (95% counting efficiency). Samples were irradiated as described under Materials and Methods. At various times, aliquots were removed and the fluorescence intensity at 410 nm was recorded (B). Intensities were relative to the intensity of the unphotolyzed (zero time) sample for each nucleotide. Fluorometer settings were as in Figure 1 except that the excitation band-pass was set to 8 nm prior to the monochrometer and narrowed to 0.5 nm prior to the sample to minimize photolysis of the sample during the measurement. Solid urea was then added to 6 M, and noncovalent radiolabel was removed by a gel filtration centrifuge column as described under Materials and Methods except that the gel was equilibrated in 6 M urea in KCl–HEPES buffer (pH 7.0). Covalent incorporation (moles of covalent nucleotide per mole of $SF_1$) was determined from the radioactivity and protein concentrations of the column effluents. These data were then converted to moles of covalent nucleotide per mole of nucleotide trapped prior to photolysis (A).

The relative contribution of static and dynamic quenching observed for the CBH probes can be estimated from the parameter $\gamma = (\tau/\tau_0)(F/F_0)$, assuming that the quantum yield of the static complex is negligible, where $\gamma$ corresponds to the fraction of absorption transitions by free, unquenched fluorophore in the ground state relative to the total number of

absorptions (Spencer et al., 1974). $F_0$ and $\tau_0$ are the quantum yield and lifetime, respectively, of εADP, and $F$ and $\tau$ are the corresponding values for the CBH derivatives. As can be seen from Tables I and II, $\gamma$ is very close to 1 for both CBHεADP and 3′(CBH)2′dεADP; i.e., $F/F_0 = \tau/\tau_0$. Thus, quenching is only by processes competitive with emission, and this excludes the presence of a nonfluorescent static complex. Thus, the lifetimes ($\tau_i$) and fractional fluorescence intensities ($f_i$) from Table II for CBHεADP can be used to calculate the mole fractions ($X_i$) of each component present in a mixture of components. For a two-component system

$$X_1 = (f_1/\tau_1)/[(f_1/\tau_1) + (f_2/\tau_2)]$$

$$X_2 = 1 - X_1$$

According to these equations and the data from Table II, $X_1 = 0.6$ and $X_2 = 0.4$, where the 25.6-ns component is $\tau_1$ and the 4.2-ns component is $\tau_2$. This result is in excellent agreement with the $^1$H NMR spectrum (not shown) which indicated that CBHεADP was an equilibrium mixture of the 3′ and 2′ isomers in a ratio of 6 to 4. The possibility of contaminating εADP contributing the 25.6-ns lifetime (Table II) of CBHεADP (59% of the fluorescence) was ruled out by HPLC and TLC analyses. Also, possible contamination of CBH with $Bz_2$ acid was ruled out by $^1$H NMR analysis of the CBH before the synthesis of CBHεADP. Therefore, the 4.2-ns lifetime of CBHεADP (Table II) cannot be due to contaminating $Bz_2$εADP.

These data in Tables I and II for the quantum yields and lifetimes of the ethenonucleotide derivatives free in buffer are in general agreement with other investigations concerning the extent of intramolecular complexing in modified coenzymes εNAD$^+$ and εFAD (Barrio et al., 1972, 1973), ethenoadenosine dinucleoside phosphates (Tolman et al., 1974), and NADH and related synthetic models (Scott et al., 1970). The $^1$H NMR and fluorescence results of Jacobson and Colman (1984) showed that in 5′-[(fluorosulfonyl)benzoyl]-1,$N^6$-ethenoadenosine (5′-FSBεA) the benzoyl moiety is intramolecularly stacked with the purine ring. Their low value for the quantum yield of 5′-FSBεA of 0.01 (1.8% of that of εADP) reveals considerable quenching of the ε-adenine ring by the benzoyl group. Although the mechanism of quenching was not established, energy transfer from the ethenoadenine ring to the benzoyl group would be consistent with the low quantum yields observed even in solvents known to favor the extended form of the analogues where static or dynamic quenching would be diminished.

*Quantum Yields and Lifetimes of Ethenonucleotides Bound and Trapped on $SF_1$.* εADP exhibits a single lifetime in solution of 26.5 ns at 6 °C (Table II). However, the fluorescence decay of trapped or reversibly bound εADP was heterogeneous; $\chi_R^2$ could consistently be reduced by a fit to two components (20.6 and 6.7 ns) with shorter lifetimes than that of εADP in solution (26.5 ns). This result was consistent with recent lifetime measurements of εADP·$SF_1$ complexes made in our laboratory (Perkins and Yount, unpublished observations) and with those of Rosenfeld and Taylor (1984). There was a small but reproducible decrease in quantum yield of εADP upon binding $SF_1$ (ratio of bound/free = 0.80) which was similar to the decrease in quantum yield (0.67) measured by Perkins and Yount (1984). εAMP-PNP gave the same result. As was reported by Perkins et al. (1984), trapping of εADP at the active site with pPDM did not further reduce the quantum yield of εADP.

The general lack of large changes in the quantum yields of the $Bz_2$ derivatives upon binding to $SF_1$ indicated that the $SF_1$ binding site probably sets only small restrictions on the relative orientations between the nucleotide base and the $Bz_2$ moiety and thus on the degree of intramolecular quenching.

Heterogeneous lifetimes were observed for the $Bz_2$ derivatives reversibly bound or trapped on $SF_1$ (Table II). A fit to two components, rather than one, typically reduced $\chi_R^2$ by a factor of 50–200 (Table II); all attempts at three-component fits did not further reduce $\chi_R^2$. The shorter lifetime component seen for the $Bz_2$ derivatives bound to $SF_1$ cannot be explained as a signal from unbound probe. On the basis of the measured binding constant (Figure 3) less than 10% of the probe was free under the experimental conditions. The results of a titration of $SF_1$ with $Bz_2$εADP (from 0.28 to 1.6 nucleotide per protein, data not shown) indicated that the progressive increase in the fractional fluorescence intensity ($f_i$) of the shorter lifetime could be accounted for by the calculated amount of free probe predicted from the law of mass action and the measured apparent dissociation constant (Figure 3). Molecular assignment of each of the two components was complicated in that the parent compound εADP had two lifetimes bound or trapped on $SF_1$ (Table II). Therefore, for the $Bz_2$ compounds, lifetime and quantum yield data were compared together to provide the most information about the fluorescent probes bound or trapped at the active site. $Bz_2$εADP and 3′($Bz_2$)2′dεADP exhibited similar lifetimes trapped or bound on $SF_1$. Thus the two lifetime components observed, one longer (12 ns) and one shorter (3 ns) than those of the respective free probes, do not correspond to either one of the 2′ or 3′ isomers. The measured quantum yields (Table I) for both the reversibly bound and trapped $Bz_2$εADP were lower than the corresponding values for 3′($Bz_2$)2′dεADP. Thus, if 3′($Bz_2$)2′dεADP binds to $SF_1$ in a conformation similar to that of the 3′ isomer of $Bz_2$εADP, the similar lifetimes for $Bz_2$εADP and 3′($Bz_2$)-2′dεADP cannot be explained by exclusive binding of the 3′ isomer of $Bz_2$εADP but would be consistent with a statically quenched 2′ isomer at the $SF_1$ binding site. Trapping further quenchs or increases the mole fraction of the 2′ isomer, as the trapped lifetimes were similar to those for bound, while the quantum yield of $Bz_2$εADP was lowered by a factor of 2.6 upon trapping (Table I). A detailed analysis of the fractional contributions from the 2′ and 3′ isomers to the quantum yields of trapped and bound $Bz_2$εADP was not attempted due to the magnitude of uncertainty in the measured quantum yields.

*Photoincorporation of pPDM-Trapped Ethenonucleotide Derivatives into $SF_1$.* Photoincorporation of [$^{14}$C]$Bz_2$εADP and 3′([$^{14}$C]$Bz_2$)2′dεADP trapped on $SF_1$ by pPDM is shown in Figure 4A. The levels of covalent incorporation, 50% and 40% of the trapped analogues, saturated after 50- and 80-min irradiation for $Bz_2$εADP and 3′($Bz_2$)2′dεADP, respectively. These values have been corrected for the nonspecific binding component of the assay which was the apparent incorporation measured at $t = 0$ (see Figure 4A). The time required to reach saturation was always longer for 3′($Bz_2$)2′dεADP than for $Bz_2$εADP. This behavior could be explained if the 2′ isomers were incorporated more rapidly than the 3′ isomers. The stability of the trapped nucleotide–$SF_1$ complexes in the dark at 4 °C was measured by the decrease in fluorescence polarization with time as nucleotide once off the enzyme did not rebind. These results (data not shown) indicated that only 2–3% of the trapped nucleotides leaked out of the active site after 1 h at 4 °C. This result was similar to the off-rate of pPDM-trapped εADP measured by Perkins et al. (1984) using the same method. The off-rates of pPDM-trapped εADP with and without photolysis were identical. Assuming a similar behavior for the $Bz_2$ nucleotides, the saturable behavior of the

Scheme I

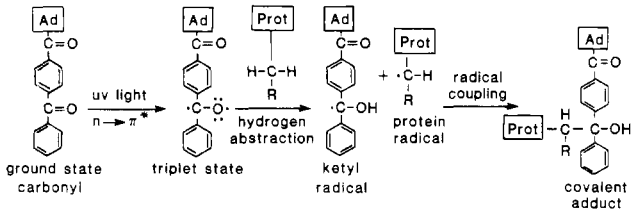


photoincorporation time courses (Figure 4) could not be explained by a photolysis-dependent leakage of the trapped nucleotides.

The irradiation-dependent increase in relative fluorescence intensity at 410 nm (Figure 4B) paralleled the increase in covalent incorporation (Figure 4A). The relative fluorescence intensities saturated at levels of 8- and 2-fold over the fluorescence of the trapped nucleotides (no irradiation) for $Bz_2\epsilon$ADP and 3′($Bz_2$)2′d$\epsilon$ADP, respectively. The differences in the fluorescence intensities at saturation for the two $Bz_2$ probes can be explained by their different quantum yields before (trapped) and after irradiation (Table I). In a control experiment using $\epsilon$ADP, the quantum yield did not change upon irradiation (Table I). In the proposed mechanism of $Bz_2$ photoincorporation [Scheme I; modified from Campbell and Gioannini (1974)], the carbonyl chromophore reacts to yield a tertiary alcohol adduct with the protein. As has been demonstrated, the quantum yields of the CBH derivatives were greater than that of the respective $Bz_2$ derivatives. Thus, the observed photolysis-dependent increase in fluorescence (Figure 4B) was consistent with a reaction of the carbonyl of $Bz_2$ with the protein to generate an adduct that can be modeled by the CBH derivatives trapped at the active site.

The quantum yield of the irradiated enzyme–analogue complex will be the sum of the quantum yields of the covalent nucleotide–protein adduct and remaining unincorporated $Bz_2\epsilon$ADP (substoichiometric labeling). A significant fluorescence contribution from unreacted $Bz_2\epsilon$ADP will complicate lifetime measurements for energy-transfer studies, as the unreacted $Bz_2\epsilon$ADP possesses a distinct lifetime. The fluorescence properties of the trapped CBH$\epsilon$ADP and the analogue of its 3′ isomer, 3′(CBH)2′d$\epsilon$ADP, have been used as spectral models of the protein–nucleotide covalent adduct to estimate the relative fluorescence contributions from each of these components after photolysis. The predicted quantum yield of irradiated $Bz_2\epsilon$ADP·$SF_1$, assuming 50% reacted and 50% unreacted as was determined from the data in Figure 4A, was 0.19 by calculation, i.e., 50% of the quantum yield of trapped $Bz_2\epsilon$ADP (0.021) added to 50% of the quantum yield of trapped CBH$\epsilon$ADP (0.36; Table I). The measured quantum yield of the irradiated enzyme–analogue complex from Table I was 0.17 ± .02. From this analysis the fluorescence of the unreacted $Bz_2\epsilon$ADP represents only ~6% of the total fluorescence of the irradiated sample. A parallel calculation for 3′($Bz_2$)2′d$\epsilon$ADP (40% reacted, 60% unreacted; see Figure 4A) predicts a quantum yield of 0.22, i.e., 60% of the quantum yield of trapped 3′($Bz_2$)2′d$\epsilon$ADP (0.12) and 40% of the quantum yield of trapped 3′(CBH)2′d$\epsilon$ADP (0.36; Table I). The measured quantum yield was 0.23 ± 0.03. From this analysis, ~33% of the total fluorescence of this irradiated sample represents the unreacted 3′($Bz_2$)2′d$\epsilon$ADP that has remained trapped on $SF_1$. For both analogues, $Bz_2\epsilon$ADP and 3′($Bz_2$)2′d$\epsilon$ADP, the predicted quantum yields from calculations based upon measured photoincorporation levels and the CBH model compounds were in excellent agreement with the measured quantum yields of the irradiated trapped nucleotides. This result implies that the remaining trapped nucleotide, which did not react covalently with the protein, was spectrally equivalent to $Bz_2\epsilon$ADP, i.e., with the keto group of $Bz_2$ unchanged. The three $Bz_2$ nucleotide probes, $Bz_2\epsilon$ADP, 3′-($Bz_2$)2′d$\epsilon$ADP, and $Bz_2$ADP (Mahmood & Yount, 1984), give about the same levels of photoincorporation. This suggests that both the 2′ and 3′ isomers can photoinsert since the trapped 3′($Bz_2$)2′d$\epsilon$ADP actually inserted at a somewhat lower level (40%) and at a lower rate than the 2′/3′ analogues. The reason for less than the theoretically possible 100% photoincorporation (see Scheme I) remains obscure but likely resides with heterogeneity in the protein rather than a nonproductive side reaction which prevents covalent insertion.

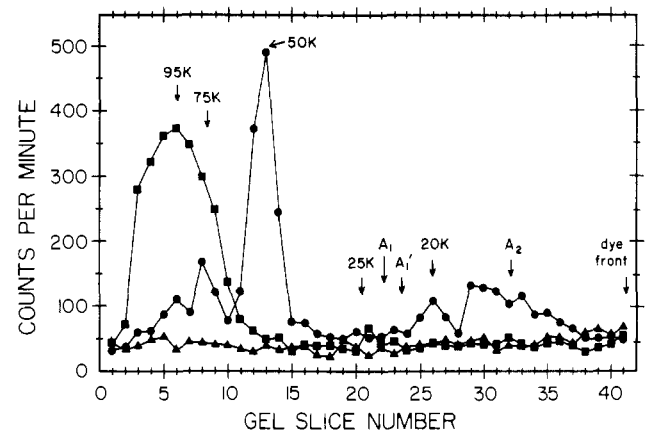


FIGURE 5: SDS–PAGE analyses of a limited tryptic digest of [$^{14}$C]$Bz_2\epsilon$ADP-labeled $SF_1$. Analytical procedures for this gel experiment are described under Materials and Methods. $SF_1$ was modified with pPDM in the presence of [$^{14}$C]$Bz_2\epsilon$ADP as described in Figure 2 and purified to remove untrapped nucleotide as described under Materials and Methods. $SF_1$ (225 $\mu$g) modified to 0.68 mol of [$^{14}$C]$Bz_2\epsilon$ADP/mol of $SF_1$ (5400 cpm/nmol) was photolyzed for 50 min (■) and digested with trypsin for 30 min (●). The positions of the tryptic fragments, indicated by arrows, were derived from the Coomassie blue staining pattern (not shown) of the photolyzed and digested sample (●). Coomassie blue stained control samples of unphotolyzed and photolyzed $SF_1$ in the absence of trapped label were not distinguishable from the three samples shown here. The total counts recovered for the photolyzed samples represent a 60 ± 5% recovery of the radioactivity applied to the gel, assuming 0.37 ± 0.02 mol of covalent label/mol of $SF_1$. The background levels in the unphotolyzed sample (▲) were not significantly higher than gel slices containing no added radiolabel (data not shown). Noncovalently bound probe migrates at the schlieren line, which is not shown on the graph.

As was shown above, the product of the photochemical reaction of $Bz_2\epsilon$ADP with $SF_1$ had a quantum yield comparable to that measured for CBH$\epsilon$ADP trapped at the active site (0.36). The lifetimes and fractional intensities of trapped $Bz_2\epsilon$ADP that has been irradiated were also comparable to those of CBH$\epsilon$ADP reversibly bound or trapped on $SF_1$ with a major (~90%) component of 20–21 ns (Table II). The lifetimes and fractional intensities of the covalently bound fluorescent nucleotide were also comparable to those of $\epsilon$ADP bound or trapped on $SF_1$. However, as seen in Table I, the quantum yield for $\epsilon$ADP trapped on $SF_1$ (0.62) is 1.7-fold higher than the calculated quantum yield of the product of the photochemical reaction of $Bz_2\epsilon$ADP with $SF_1$ (0.36), indicating that a statically quenched moiety is present in the trapped CBH$\epsilon$ADP and the irradiated $Bz_2\epsilon$ADP·$SF_1$ samples. The magnitude of this quenching did not appear to depend upon the position of the CBH on the ribose ring, as both the 2′ and 3′ isomers of CBH$\epsilon$ADP had the same quantum yields (0.36) trapped on $SF_1$ (Table I).

*Identification of Tryptic Peptide(s) Modified by Photoaffinity Labeling.* Covalently labeled $SF_1$ was digested briefly with trypsin, and the major peptide(s) photolabeled by

irradiation of trapped [$^{14}$C]$Bz_2\epsilon$ADP was (were) identified by gel electrophoresis (Figure 5). Without photolysis no increased radioactivity was seen throughout the gel. However, after irradiation, all of the $^{14}$C was detected in a broad band (due to an overloaded lane) corresponding to the 95-kDa heavy chain fragment, as determined from its position in a lane stained with Coomassie blue (not shown). The radioactivity comigrating with either of the alkali light chains, $A_1$ or $A_2$, was at background level. Further limited trypsin digestion of this sample shows the 95-kDa heavy chain fragment cleaved to the characteristic 75-, 50-, 25-, and 20-kDa fragments (Balint et al., 1978), where the 75-kDa polypeptide is the precursor to the 50- and 25-kDa fragments. The profile of radioactivity (Figure 5) shows that [$^{14}$C]$Bz_2\epsilon$ADP primarily labeled the 50-kDa tryptic fragment or its 75-kDa precursor. The 25-kDa peptide and its precursor 27-kDa peptide contained only background radioactivity. The apparent labeling of the $A_2$ light chain after trypsinization must have resulted from comigrating tryptic fragments of the labeled 95-kDa heavy chain since no apparent $A_2$ labeling was present prior to trypsin digestion. The 20-kDa fragment was slightly labeled (4.5% of the total recovered counts). These results indicated very specific labeling of the 50-kDa peptide; ~80% of the radioactivity of the trypsin-treated sample was associated with the 75- and 50-kDa fragments. We obtained an identical result using 3′([$^{14}$C]$Bz_2$)2′d$\epsilon$ADP in the same experiment (data not shown). The results of a similar experiment using nonfluorescent [$^3$H]$Bz_2$ADP trapped on $SF_1$ (Mahmood & Yount, 1984) were nearly identical with those presented in Figure 5. Thus, three different $Bz_2$ analogues have been used to photolabel the active site region of $SF_1$; all three photoprobes label predominantly the 50-kDa peptide. These results indicate that the $Bz_2$ analogues label a portion of the 50-kDa peptide which is within 6–7 Å of the active site.

In conclusion, $Bz_2\epsilon$ADP, a photoactivatable derivative of the fluorescent nucleotide $\epsilon$ADP, has been synthesized and chemically characterized. CBH$\epsilon$ADP, a spectral analogue of the product of the photochemical reaction of $Bz_2\epsilon$ADP with $SF_1$, has also been synthesized and characterized. $^1$H NMR indicated both analogues were a mixture of the 3′ (60%) and 2′ (40%) isomers. In addition, 3′($Bz_2$)2′d$\epsilon$ADP and 3′-(CBH)2′d$\epsilon$ADP have been synthesized as analogues of the 3′ isomers of $Bz_2\epsilon$ADP and CBH$\epsilon$ADP, respectively. All four ethenonucleotide derivatives are stably and noncovalently trapped at the active site of $SF_1$ by the bifunctional thiol cross-linker pPDM in a similar manner to ADP and $\epsilon$ADP. Steady-state and time-resolved fluorescence techniques have been used to study the intramolecular quenching mechanisms for the four new etheno derivatives free in solution and bound to the $SF_1$ active site. $Bz_2\epsilon$ADP and 3′($Bz_2$)2′d$\epsilon$ADP trapped on $SF_1$ by pPDM were shown to photoincorporate specifically and with high efficiency (40–50%) into the active site of $SF_1$. Fluorescence techniques were used to investigate the mechanism of the photochemical reaction of the $Bz_2$ nucleotides with the active site region of $SF_1$. Limited trypsin digestion of the irradiated nucleotide–$SF_1$ samples indicated specific labeling of the 50-kDa peptide fragment of the heavy chain. In other experiments (Cremo & Yount, 1987), $Bz_2\epsilon$ADP-labeled $SF_1$ has been shown to bind to F-actin. Thus $Bz_2\epsilon$ADP-labeled $SF_1$ will be valuable as a donor in distance measurements by fluorescence resonance energy transfer to acceptor sites on actin and as a general probe of the $SF_1$ active site.

## ACKNOWLEDGMENTS

We thank Jean Grammer, Riaz Mahmood, Ed Huston, Gerhard Munske, William Perkins, Jurgen Weiel, Don Appel, and Kay Nakamaye for invaluable technical advice and assistance and Jane Peterson for preparation of the manuscript. We especially thank Dr. Enrico Gratton for supplying the heterogeneity analysis software (Least-Squares Analysis Version ISSC6).

**Registry No.** CBH, 579-52-2; CBH·$x$K, 110698-25-4; ATPase, 9000-83-3; $\epsilon$ADP, 38806-39-2; pPDM, 3278-31-7; [2,8-$^3$H]$\epsilon$ADP, 110682-78-5; $Bz_2\epsilon$ADP, 110682-84-3; [$^3$H]$Bz_2\epsilon$ADP, 110682-85-4; [$^{14}$C]$Bz_2\epsilon$ADP, 110682-86-5; CBH$\epsilon$ADP, 110682-87-6; 3′($Bz_2$)-2′d$\epsilon$ADP, 110682-79-6; 3′([$^{14}$C]$Bz_2$)2′d$\epsilon$ADP, 110682-80-9; 2′d$\epsilon$ADP·$x$NBu$_3$, 110682-82-1; 3′(CBH)2′d$\epsilon$ADP, 110682-83-2; 3′(CBH)2′d$\epsilon$ADP·$x$Na, 110698-26-5; $Bz_2$ acid, 611-95-0; [$^{14}$C]$Bz_2$ acid, 101025-06-3.

## REFERENCES

Abeijon, C., Capasso, J. M., Tal, D., Vann, W. F., & Hirschberg, C. B. (1986) *J. Biol. Chem. 261*, 11374–11377.

Ames, B. N., & Dubin, D. T. (1960) *J. Biol. Chem. 235*, 769–777.

Balint, M., Wolf, I., Tarcsafalvi, A., Gergely, J., & Sreter, F. A. (1978) *Arch. Biochem. Biophys. 190*, 793–799.

Barrio, J. R., Secrist, J. A., III, & Leonard, N. J. (1972) *Proc. Natl. Acad. Sci. U.S.A. 69*, 2039–2045.

Barrio, J. R., Tolman, G. L., Leonard, N. J., Spencer, R. D., & Weber, G. (1973) *Proc. Natl. Acad. Sci. U.S.A. 70*, 941–946.

Bhandari, D. G., Trayer, H. R., & Trayer, I. P. (1985) *FEBS Lett. 187*, 160–166.

Botts, J., Takashi, R., Torgerson, P., Hozumi, T., Muhlrad, A., Mornet, D., & Morales, M. F. (1984) *Proc. Natl. Acad. Sci. U.S.A. 81*, 2060–2064.

Bradford, M. M. (1976) *Anal. Biochem. 72*, 248–254.

Burke, M. (1980) *Arch. Biochem. Biophys. 203*, 190–194.

Burke, M., & Reisler, E. (1977) *Biochemistry 16*, 5559–5563.

Campbell, P., & Gioannini, T. L. (1979) *Photochem. Photobiol. 29*, 883–892.

Chalovich, J. M., Greene, L. E., & Eisenberg, E. (1983) *Proc. Natl. Acad. Sci. U.S.A. 80*, 4909–4913.

Cremo, C., & Yount, R. G. (1987) *Biophys. J. 51*, 485a.

Dalbey, R. E., Weiel, J., Perkins, W. J., & Yount, R. G. (1984) *J. Biochem. Biophys. Methods 9*, 251–266.

Dos Remedios, C. G., & Cooke, R. (1984) *Biochim. Biophys. Acta 788*, 193–205.

Galardy, R. E., Craig, L. C., & Printz, M. P. (1973) *Nature (London) New Biol. 242*, 127–128.

Gilman, H., & Blatt, A. H., Eds. (1941) *Organic Syntheses*, Collect. Vol. I, p 90, Wiley, New York.

Gottikh, B. P., Krayevsky, A. A., Tarussova, N. B., Purygin, P. P., & Tsilevich, T. L. (1970) *Tetrahedron 26*, 4419–4433.

Grammer, J. C., Czarnecki, J. J., & Yount, R. G. (1985) *Biophys. J. 47*, 306a.

Gratton, E., Limkeman, M., Lakowicz, J. R., Maliwal, B. P., Cherek, H., & Laczko, G. (1984) *Biophys. J. 46*, 479–486.

Griffin, B. E., Jarman, M., Reese, C. B., Sulston, J. E., & Trentham, D. R. (1966) *Biochemistry 5*, 3638–3649.

Guillory, R. J., & Jeng, S. J. (1977) *Methods Enzymol. 46*, 259–288.

Haugland, R. P., Yguerabide, J., & Stryer, L. (1969) *Proc. Natl. Acad. Sci. U.S.A. 63*, 23–30.

Hiratsuka, T. (1983) *Biochim. Biophys. Acta 742*, 496–550.

Hoard, D. E., & Ott, D. G. (1965) *J. Am. Chem. Soc. 87*, 1785–1789.

Jacobson, M. A., & Colman, R. F. (1984) *J. Biol. Chem. 259*, 1454–1460.

Kambouris, N. G., & Hammes, G. G. (1985) *Proc. Natl. Acad. Sci. U.S.A. 82*, 1950–1953.

Laemmli, U. K. (1970) *Nature (London) 227*, 680–685.
Lakowicz, J. R. (1983) in *Principles of Fluorescence Spectroscopy*, p 324, Plenum, New York.
Lakowicz, J. R., Cherek, H., & Bevan, D. R. (1980) *J. Biol. Chem. 255*, 4403–4406.
Lakowicz, J. R., Cherek, H., & Balter, S. (1981) *J. Biochem. Biophys. Methods 5*, 131–146.
Lakowicz, J. R., Laczko, G., Cherek, H., Gratton, E., & Limkeman, M. (1984) *Biophys. J. 46*, 463–477.
Leonard, N. J. (1984) *CRC Crit. Rev. Biochem. 15*, 125–199.
Mahmood, R., & Yount, R. G. (1984) *J. Biol. Chem. 259*, 12956–12959.
Mahoney, C. W., & Yount, R. G. (1984) *Anal. Biochem. 138*, 246–251.
McLaughlin, C. S., & Ingram, V. M. (1965a) *Biochemistry 4*, 1442–1447.
McLaughlin, C. S., & Ingram, V. M. (1965b) *Biochemistry 4*, 1448–1456.
Miki, M., & Wahl, P. (1984) *Biochim. Biophys. Acta 790*, 275–283.
Morales, M. F., Borejdo, J., Botts, J., Cooke, R., Mendelson, R. A., & Takashi, R. (1982) *Annu. Rev. Phys. Chem. 33*, 319–351.
Munson, K. B., Smerdon, M. J., & Yount, R. G. (1986) *Biochemistry 25*, 7640–7650.
Nakamaye, K. L., & Yount, R. G. (1985) *J. Labelled Compd. Radiopharm. 22*, 607–613.
Nakamaye, K. L., Wells, J. A., Bridenbaugh, R., Okamoto, Y., & Yount, R. G. (1985) *Biochemistry 24*, 5226–5235.
Parker, C. A., & Reese, W. T. (1960) *Analyst (London) 85*, 587–600.
Penefsky, H. S. (1977) *J. Biol. Chem. 252*, 2891–2899.
Perkins, W. J., Wells, J. A., & Yount, R. G. (1984) *Biochemistry 23*, 3994–4002.
Rajkowski, K. M., & Cittanova, N. (1981) *J. Theor. Biol. 93*, 691–696.
Reisler, E. (1982) *Methods Enzymol. 95*, 84–92.
Rosenfeld, S. S., & Taylor, E. W. (1984) *J. Biol. Chem. 259*, 11920–11929.
Scatchard, G. (1949) *Ann. N.Y. Acad. Sci. 51*, 660–671.
Scott, T. G., Spencer, R. D., Leonard, N. J., & Weber, G. (1970) *J. Am. Chem. Soc. 92*, 687–695.
Secrist, J. A., III, Barrio, J. R., Leonard, N. J., & Weber, G. (1972) *Biochemistry 11*, 3499–3506.
Spencer, R. D., & Weber, G. (1970) *J. Chem. Phys. 52*, 1654–1663.
Spencer, R. D., Weber, G., Tolman, G. L., Barrio, J. R., & Leonard, N. J. (1974) *Eur. J. Biochem. 45*, 425–429.
Sutoh, K., Yamamoto, K., & Wakabayashi, T. (1986) *Proc. Natl. Acad. Sci. U.S.A. 83*, 212–216.
Takashi, R. (1979) *Biochemistry 18*, 5164–5169.
Tolman, G. L., Barrio, J. R., & Leonard, N. J. (1974) *Biochemistry 13*, 4869–4878.
Trayer, H. R., & Trayer, I. P. (1983) *Eur. J. Biochem. 135*, 47–59.
Trayer, H. R., Prince, H. P., Levine, B. A., & Trayer, I. P. (1982) *J. Muscle Res. Cell Motil. 3*, 462–467.
Turro, N. J. (1978) *Modern Molecular Photochemistry*, Benjamin/Cummings, Reading, MA.
Vibert, P., & Craig, R. (1982) *J. Mol. Biol. 157*, 299–304.
Vibert, P., Szentkiralyi, E., Hardwicke, P., Szent-Giorgyi, A. G., & Cohen, C. (1986) *Biophys. J. 49*, 131–133.
Wagner, P. D., & Yount, R. G. (1975) *Biochemistry 14*, 1900–1907.
Wagner, P. D., & Weeds, A. G. (1977) *J. Mol. Biol. 109*, 455–473.
Weber, G. (1952) *Biochem. J. 51*, 145–148.
Weeds, A. G., & Taylor, R. S. (1975) *Nature (London) 257*, 54–56.
Wells, J. A., & Yount, R. G. (1979) *Proc. Natl. Acad. Sci. U.S.A. 76*, 4966–4970.
Wells, J. A., & Yount, R. G. (1980) *Biochemistry 19*, 1711–1717.
Wells, J. A., & Yount, R. G. (1982) *Methods Enzymol. 95*, 93–116.
Wells, J. A., Werber, M. M., Legg, J. I., & Yount, R. G. (1979a) *Biochemistry 18*, 4793–4799.
Wells, J. A., Werber, M. M., & Yount, R. G. (1979b) *Biochemistry 18*, 4800–4805.
Wells, J. A., Sheldon, M., & Yount, R. G. (1980) *J. Biol. Chem. 255*, 1598–1602.
Williams, N., & Coleman, P. S. (1982) *J. Biol. Chem. 257*, 2834–2841.
Winkelmann, D. A., Mekeel, H., & Rayment, I. (1985) *J. Mol. Biol. 181*, 487–493.
Zincke, T. (1872) *Justus Liebigs Ann. Chem. 161*, 102.